HHS Public Access

Author manuscript

Behav Brain Res. Author manuscript; available in PMC 2018 March 01.

Published in final edited form as:

Behav Brain Res. 2017 March 01; 320: 119–127. doi:10.1016/j.bbr.2016.12.003.

Frequency-dependent, transient effects of subthalamic nucleus deep brain stimulation on methamphetamine-induced circling and neuronal activity in the hemiparkinsonian rat

Rosa Q. So[1], **George C. McConnell**[1], and **Warren M. Grill**[1,2,3,*]

[1]Department of Biomedical Engineering, Duke University, Durham NC USA

[2]Department of Electrical and Computer Engineering, Duke University, Durham NC USA

[3]Department of Neurobiology, Duke University, Durham NC USA

Abstract

Methamphetamine-induced circling is used to quantify the behavioral effects of subthalamic nucleus (STN) deep brain stimulation (DBS) in hemiparkinsonian rats. We observed a frequency-dependent transient effect of DBS on circling, and quantified this effect to determine its neuronal basis. High frequency STN DBS (75 – 260 Hz) resulted in transient circling contralateral to the lesion at the onset of stimulation, which was not sustained after the first several seconds of stimulation. Following the transient behavioral change, DBS resulted in a frequency-dependent steady-state reduction in pathological ipsilateral circling, but no change in overall movement. Recordings from single neurons in globus pallidus externa (GPe) and substantia nigra pars reticulata (SNr) revealed that high frequency, but not low frequency, STN DBS elicited transient changes in both firing rate and neuronal oscillatory power at the stimulation frequency in a subpopulation of GPe and SNr neurons. These transient changes were not sustained, and most neurons exhibited a different response during the steady-state phase of DBS. During the steady-state, DBS produced elevated neuronal oscillatory power at the stimulus frequency in a majority of GPe and SNr neurons, and the increase was more pronounced during high frequency DBS than during low frequency DBS. Changes in oscillatory power during both transient and steady-state DBS were highly correlated with changes in firing rates. These results suggest that distinct neural mechanisms were responsible for transient and sustained behavioral responses to STN DBS. The transient contralateral turning behavior following the onset of high frequency DBS was paralleled by transient changes in firing rate and oscillatory power in the GPe and SNr, while steady-state suppression of ipsilateral turning was paralleled by sustained increased synchronization of basal ganglia neurons to the stimulus pulses. Our analysis of distinct frequency-dependent transient and steady-state responses to DBS lays the foundation for future mechanistic studies of the immediate and persistent effects of DBS.

[*]Corresponding author, Address all correspondence to: Warren M. Grill, Ph.D., Department of Biomedical Engineering, Box 90281, Duke University, Durham NC USA 27708-0281, warren.grill@duke.edu, (919) 660-5276 Phone, (919) 684-4488 FAX.

1. Introduction

Subthalamic nucleus (STN) deep brain stimulation (DBS) is an effective treatment for the motor symptoms of Parkinson's disease (PD) (Moro et al. 2010), but the mechanisms of action of DBS remain unclear. The unilaterally-6-OHDA-lesioned rat model of PD is commonly used in DBS studies (Spieles-Engemann et al. 2010; Nowak et al. 2011), and methamphetamine-induced circling behavior is used to quantify effects of DBS (Meissner et al. 2002; Gradinaru et al. 2009). Administration of methamphetamine in unilaterally-lesioned rats results in circling ipsilateral to the lesion (Ungerstedt and Arbuthnott 1970), and STN DBS reverses this behavior, depending on the amplitude, frequency, pattern and location of stimulation (So et al. 2012; McConnell et al. 2012; Summerson et al. 2014; McConnell et al. 2016).

In the course of our experiments, we observed a transient behavioral effect of STN DBS – rats sharply reversed the direction of circling at the onset of high frequency stimulation, exhibiting a brief bout of circling contralateral to the lesion. Prior studies averaged the behavioral and neuronal effects of DBS across time (Burbaud et al. 1994; Shi et al. 2006; Moran et al. 2011), and did not consider transient changes at the onset of DBS. Therefore, we quantified this transient behavioral effect of DBS as a function of stimulation frequency, and analyzed single unit neuronal activity from the basal ganglia to determine the neuronal basis for transient contralateral circling. Such time-dependent changes in behavior and neural activity may shed light on the differential time-dependent effects of STN DBS on symptoms in persons with PD (Temperli et al. 2003; Lopiano et al. 2003; Kereztenyi et al. 2007; Cooper et al. 2011).

2. Methods

2.1. Implantation of stimulating and recording electrodes

We conducted stereotactic surgery in Long Evans rats (250 g – 300 g, n=11) under 2 % isoflurane anesthesia using coordinates from the rat brain atlas (Paxinos & Watson, 2005). All animal care and experimental procedures were approved by the Duke University Institutional Animal Care and Use Committee. Each rat was implanted with a 2-by-2 platinum-iridium stimulating microelectrode array (impedance of 10 kΩ) in the STN [A 3.6 mm from bregma; L 2.6 mm; H 6.6 – 6.9 mm], and 4-by-4 stainless steel microwire recording arrays (impedance of 0.5 MΩ) in globus pallidus externa (GPe) [A 1.0 mm from bregma; L 3.0 mm; H 5.4 mm] and substantia nigra pars reticulata (SNr) [A 4.2 mm from bregma; L 2.3 mm; H 7.2 mm]. A cannula was implanted into the medial forebrain bundle (MFB) [A 2.0 mm from bregma; L 2.0 mm; H 7.5 mm]. After one week of recovery, rats were again anesthetized with 2 % isoflurane, and a unilateral lesion of the substantia nigra pars compacta (SNc) was made by infusing 10 μl of 6-OHDA (10 mM) into the MFB at a rate of 2 μl/min. Thirty minutes prior to lesioning, rats were pretreated with 50 mg/kg, i.p., pargyline (Sigma-Aldrich) to inhibit monoamine oxidase and 5 mg/kg, i.p., desipramine (Sigma-Aldrich) to protect noradrenergic neurons. Rats recovered for one week before commencing behavioral experiments. All of the rats used in this study were also used in other studies: So et al. 2012 – 7 out of 16 rats; McConnell et al. 2012 – 11 out of 13 rats; McConnell et al. 2016 – 10 out of 11 rats. Only rats that had recording electrodes within

GPe and/or SNr as confirmed with postmortem histology were included in the present study, as these animals provided both behavioral and electrophysiological data.

2.2. Quantifying effects of DBS on methamphetamine-induced circling

Changes in behavior during different frequencies (10 – 260 Hz) of STN DBS were quantified using methamphetamine-induced circling in 11 rats. During each experiment, the rat was administered methamphetamine (1.25 – 1.875 mg/kg, i.p.) and placed in a dark 30-cm-diameter cylindrical chamber equipped with an infrared video camera that recorded the rat's activity for two hours. During this time, bipolar stimulation (range: 30–90 μA; mean ± SD: 60.9 ± 6.8 μA) was delivered between two electrodes on the array, with at least one of the electrodes confirmed on post-mortem histology to lie within the STN. The amplitude of stimulation was determined before the start of each experiment based on sustained motor responses (decreased ipsilateral turning, increased contralateral turning, increased activity, and increased rearing) and the lack of side effects including involuntary muscle contractions of the limbs and neck during 130 Hz stimulation. Stimulation was delivered in four blocks of ten different stimulation frequencies, with presentation order randomized within each block. One minute epochs of stimulation were delivered with two minutes off between epochs. The angular velocity was sampled at 30 Hz (Clever Systems Inc., Reston, VA) and a 100 point smoothing filter was applied. Transient responses were defined as the behavioral changes measured during the first 15 s after DBS onset, while steady state responses were defined as the behavioral changes measured between 15 s and 60 s after DBS onset. The demarcation between transient and steady state responses was determined from plots of angular velocity as a function of time during 130 Hz DBS (figure 1, inset), which showed that the transient behavioral effects lasted on average approximately 15 s.

2.3. Recordings and analysis of single unit activity in the basal ganglia

Single unit neural activity was recorded in 11 rats while the rats were awake and at rest, using a multichannel acquisition processor (MAP) system (Plexon Inc., Dallas, TX). Detailed descriptions of signal processing and examples of isolation of single units have been previously described (McConnell et al. 2012; McConnell et al. 2016). Briefly, 32 channels (16 channels in GPe and 16 channels in SNr; gain = 10,000 – 25,000; filter = 150 Hz – 8.8 kHz; sampling rate = 40 kHz) were recorded simultaneously for 15 min: 5 min pre-stimulation, 5 min during DBS at one of six different frequencies, and 5 min post-stimulation. The order of DBS frequencies presented to each rat was randomized. Single units were sorted online based on waveform shapes, and the sorting was refined after each recording session using principal component analysis (Offline Sorter, Plexon Inc., Dallas, TX). The duration of the stimulation artifact for each recorded unit, ranging from 0.5–2 ms, was identified from post-stimulus time histograms (PSTHs), which showed a period of no activity following each stimulus pulse. A blanking mask was applied to pre-stimulation and post-stimulation periods to avoid any bias due to data lost to blanking during the stimulation period by artificially constructing stimulation timestamps corresponding to DBS frequency during the stimulation period and removing spikes coinciding with the blanking mask.

Spike times of sorted single units were exported and analyzed using MATLAB. The firing rate of each neuron was quantified across time (0.5 s time windows). Spectral analysis of

spike times (Mitra and Bokil 2008) was used to quantify changes in the oscillatory neuronal activity across time (0.5 s time windows; time-bandwidth product = 3; no. of tapers = 5; Chronux version 2.00). During DBS, neuronal spiking was often driven by the stimulus pulses and spike times oscillated at the stimulation frequency (figure 2A). We were interested in how neural oscillations at the stimulation frequency changed during both transient and steady state periods of stimulation. Oscillatory power in specific frequency bands of interest (stimulation frequency ± 1 Hz, e.g. 129–131 Hz for 130 Hz DBS) was calculated by taking the average power within these bands. Band sizes of 4 Hz (128–132 Hz) or 8 Hz (126–134 Hz) resulted in similar trends in the results to the 2 Hz band.

We quantified oscillatory power at the stimulation frequency during both the transient and steady-state periods of DBS to classify neuronal responses. Neurons were classified as having a transient response if there was a significant increase or decrease (one-way ANOVA, $p < 0.05$) in oscillatory power during the first 15 s of 130 Hz DBS compared to both DBS off and steady-state DBS. Steady-state effects were measured as neuronal responses after the initial transient period, and neurons were classified as having a steady-state response if the oscillatory power between 15 s and 60 s after the start of 130 Hz DBS was significantly different compared to DBS off. The same subsets of neurons were then analyzed for changes in oscillatory power and firing rate during transient and steady state stimulation at different frequencies.

2.4. Histology to evaluate dopaminergic cell loss and electrode positions

The methods used to evaluate dopaminergic cell loss and electrode positions were as previously described (So et al. 2012). Rats were deeply anesthetized with pentobarbital (100 mg/kg, i.p.), and intracardiac perfusion was conducted with 10 % formalin. The brain was postfixed overnight in 10 % formalin and sectioned coronally at 50 μm. Tyrosine hydroxylase (TH) immunohistochemistry was used to evaluate the extent of degeneration of dopaminergic neurons (So et al. 2012; McConnell et al. 2012; McConnell et al. 2016). The percentage of dopaminergic cell loss was determined by counting TH stained SNc cells on both the lesioned and non-lesioned sides under a light microscope. Cytochrome oxidase staining was used to identify the STN, GPe and SNr, and to locate stimulating and recording electrode tracks (So et al. 2012; McConnell et al. 2012; McConnell et al. 2016).

2.5. Statistical analysis

Statistical differences between conditions were determined using one-way repeated measures analysis of variance (ANOVA). After a significant factor was found, Fisher's protected least significance difference (PLSD) test was used for post-hoc pairwise comparisons. Pearson's chi-squared test was used to compare changes in proportions of neurons with increased, decreased or no change in power during transient and steady-state DBS. Finally, correlation between changes in power and firing rates were quantified using Pearson's linear correlation coefficient, and significance was tested using a Student's t distribution for a transform of the correlation. Results were considered significant at $p < 0.05$.

3. Results

All 11 rats had greater than 90 % loss of dopaminergic cells in the SNc of the lesioned hemisphere. In all rats, at least one of the pair of STN electrodes used for bipolar stimulation was within the STN. We obtained single unit recordings from a total of 62 GPe neurons (7 out of 11 rats) and 51 SNr neurons (7 out of 11 rats).

3.1 Transient and steady-state effects of DBS on behavior were frequency-dependent

The angular velocity (AV) of methamphetamine-induced circling during ten different frequencies of STN DBS was quantified over time (figure 1). Low frequency 5 Hz to 15 Hz DBS did not result in either a transient or steady-state change in AV compared to the no stimulation condition. Between 20 Hz and 30 Hz, DBS gradually reduced steady-state AV, but no transient effect was observed at the onset of stimulation. At the onset of DBS at frequencies between 75 Hz and 260 Hz, there was a transient negative AV, indicating contralateral circling (~2 contralateral rotations) during the first several seconds of DBS, and the magnitude of the transient response increased with increasing DBS frequency (figure 1B). This transient effect was followed by a sustained (steady-state) reduction in AV (i.e., reduced ipsilateral circling), especially at frequencies of 130 Hz and above, demonstrating that high frequency DBS effectively suppressed pathological turning (figure 1C). Although high frequency DBS reduced AV, the total distance traveled during stimulation was not significantly affected by DBS at any frequency of stimulation (one-way repeated measures ANOVA, $p = 0.1379$). This important control indicates that the reductions in AV during DBS were not the result of freezing or a reduction in overall movement, but rather reflect specific changes in circling behavior resulting from DBS. The effect of DBS frequency on the transient circling response (figure 1B) was comparable whether the transient time window was selected as 7 s, 10 s, or 15 s.

3.2 Transient and steady-state effects of DBS on neuronal firing were frequency-dependent

The responses of single units in GPe and SNr to 130 Hz DBS were used to characterize the transient and steady-state changes in oscillatory power and firing rate during DBS (figure 2). Of the 62 GPe units recorded across 7 rats, 21 units (34%) exhibited a transient increase in oscillatory power, 9 units (15%) exhibited a transient decrease in oscillatory power, and the remaining units exhibited no transient change in oscillatory power at the onset of 130 Hz DBS (figure 2B). In the steady state, 35 GPe units (56%) exhibited an increase in oscillatory power and 23 units (37%) exhibited a decrease in oscillatory power (figure 2B). The proportion of neurons in the steady-state with increased, no change, and decreased oscillatory power was significantly different from the transient phase (Pearson's chi-squared test, $p < 0.001$). We further classified individual units according to whether or not their steady-state response differed from their transient response (figure 2A). 15 GPe units (24%) had the same type of response (12 increased and 3 decreased in power), while 12 units (19%) had the opposite response to stimulation during the transient and steady-state periods. Comparable proportions of GPe neurons exhibited changes in oscillatory power (figure 2B) whether the transient time window was selected as 7 s, 10 s, or 15 s. These same subsets of neurons were used subsequently to analyze changes in oscillatory power and firing rate in the GPe at other stimulation frequencies (see below; figures 3A, 4A, 4B).

Of the 51 SNr units recorded across 7 rats, 16 units (31%) exhibited a transient increase in oscillatory power at the start of 130 Hz DBS, 11 units (22%) exhibited a transient decrease in oscillatory power, and the remaining units exhibited no transient change in oscillatory power (figure 2C). In the steady state 35 SNr units (69%) exhibited an increase in oscillatory power and 15 units (29%) exhibited a decrease in oscillatory power at steady state (figure 2C). The proportion of neurons in the steady-state with increased, no change, and decreased oscillatory power was significantly different from the transient phase (Pearson's chi-squared test, $p < 0.001$). 16 units (31%) had the same type of response (12 increased and 4 decreased in power), while 11 units (22%) had the opposite response to stimulation during the transient and steady-state periods (figure 2A). Comparable proportions of SNr neurons exhibited changes in oscillatory power (figure 2C) whether the transient time window was selected as 7 s, 10 s, or 15 s. These same subsets of neurons were used subsequently to analyze changes in oscillatory power and firing rate in the SNr at other stimulation frequencies (see below; figures 3B, 4C, 4D).

The subset of GPe neurons with transient increases in power at the onset of 130 Hz DBS only exhibited the transient response at DBS frequencies of 30 Hz and above, and the transient increases in power were greater and more pronounced than steady state changes in power at higher frequencies of stimulation (figures 3A, 4A). Within this subset of neurons, there was a transient increase in firing rate only during high frequency stimulation (130 Hz and 185 Hz), which was not sustained at steady state (figure 4B). On the other hand, there was no consistent DBS frequency-dependent trend for transient decreases in power or firing rate in GPe neurons. The subpopulation of neurons showing increased power in the steady-state showed a greater increase in power during high frequency DBS, which paralleled an increase in firing rate. Neurons with a decrease in power in the steady-state also showed a decrease in firing rates only at stimulation frequencies of 130 Hz and above (figure 4B). Across the whole population of GPe neurons, the changes in power during both the transient and steady-state phases of DBS were strongly correlated with changes in rate of firing (figure 5A, $p < 0.001$).

The pattern for SNr neurons exhibiting transient increases in power was similar to that of GPe neurons (figures 3B, 4C). However, there was no increase in firing rate with increasing stimulation frequency during the transient phase in this group of neurons (figure 4D). Unlike in the GPe, there was a frequency-dependent effect in the subset of neurons with transient decreases in power, with only high frequencies of DBS above 75 Hz resulting in a significant decrease in both oscillatory power and firing rate during the transient period (figures 4C–4D). At steady-state, the effect of DBS on SNr neurons was similar to GPe neurons, except there was no increase in firing rate in the group of neurons showing steady-state increases in power. A prominent decrease in steady-state firing rate during high frequency DBS was observed in the subpopulation of SNr neurons with a decrease in steady-state oscillatory power (figure 4D). Considering the entire population of SNr neurons, changes in power again showed a significant correlation with changes in firing rate during both the transient and steady-state phases of DBS (figure 5B, $p < 0.001$).

4. Discussion

We observed both transient and sustained behavioral and neuronal responses to STN DBS that were dependent on stimulation frequency. Only high frequency DBS (≥ 75 Hz) elicited a transient behavioral response, characterized by an immediate reversal of turning direction during methamphetamine-induced circling at the onset of stimulation. Further, high frequency DBS produced a sustained reduction in circling ipsilateral to the lesion, and during the steady-state phase of DBS, stimulation frequencies ≥ 130 Hz suppressed pathological turning more effectively than lower frequencies.

There were a number of differences between frequency-dependent transient and steady-state neural responses. First, the proportion of neurons in both the GPe and SNr showing a transient change in oscillatory power during high frequency DBS was less than the proportion showing steady-state changes in oscillatory power. This difference indicates that not all neurons exhibited transient changes in oscillatory activity, and more neurons exhibited a response during the steady-state phase of DBS. Many neurons also reversed their response (either from an increase to decrease or a decrease to increase in oscillatory power) during the steady-state phase compared to the transient phase. Second, in subsets of neurons with transient increases or decreases in oscillatory power and firing rates during high frequency stimulation, the changes were not sustained, or were much less pronounced during the steady-state phase. Finally, subpopulations of neurons with steady-state changes in oscillatory power often did not show a significantly different or more pronounced effect during the transient phase. These results suggest that there was a subgroup of neurons that exhibited unique changes in firing patterns during the first several seconds after the onset of high frequency DBS. Following this initial transient response, many of these neurons changed their response to stimulation while another distinct group of neurons began to respond to stimulation. These changes in power were highly correlated with changes in firing rate during both the transient and steady-state phases, indicating that the changes in oscillatory power, or synchronization to the stimulus, described above were accompanied by similar increases or decreases in firing rates.

The trends in neural response were not identical in the GPe and the SNr. In the GPe, high frequency DBS elicited a pronounced increase in oscillatory power and firing rates, during both the transient and steady state phases. In the SNr, neurons experienced either transient increases or decreases in oscillatory power during high frequency DBS, but only the latter group had a significant decrease in transient firing rate. In the steady-state, the subpopulation of neurons with increases in oscillatory power did not experience an increase in firing rate, but others with slight decreases in oscillatory power showed a pronounced decrease in firing rate.

There was a clear correlation between stimulation frequency-dependent changes in behavior and neuronal activity during both transient and steady-state phases of STN DBS. High frequency, but not low frequency, STN DBS elicited a transient behavioral change at the onset of stimulation, and the neuronal basis for this response was a brief change in activity within a subset of neurons in both the GPe and SNr. Many of the neurons in these basal ganglia nuclei exhibited a brief surge in oscillatory power during DBS onset, which means

that for several seconds, these neurons were highly synchronized and driven by the stimulus. A transient increase in synchronous firing within the GPe and SNr at the onset of high frequency STN DBS could cause GABA release within the SNc, resulting in transient contralateral turning behavior. Both the GPe and SNr make inhibitory GABAergic projections to the SNc (Smith and Bolam 1990; Iribe et al. 1999), and infusion of GABA agonists in the SNc evokes dopamine release in the ipsilateral striatum of rats, leading to contralateral turning toward the site of infusion (Martin and Haubrich 1978; Kuriyama and Kurihara 1981). Within the SNr, a subset of neurons exhibited a transient decrease in power accompanied by a transient decrease in firing rate. These changes may be explained by the direct inhibitory connections from the GPe to the SNr. Transient increases in synchronized firing within the GPe may have suppressed firing temporarily in these SNr neurons. The mechanisms underlying the transient nature of activity changes in these subgroups of basal ganglia neurons in response to high frequency STN DBS is unclear, but these responses may reflect synaptic depletion caused by high frequency DBS (Urbano et al. 2002), transient changes in membrane excitability (Raimondo et al. 2012), or some combination thereof. One shortcoming of this study is that neural recording was not performed following methamphetamine injections, and therefore the effect of methamphetamine on neural firing is not clear.

The steady-state frequency-dependent behavioral and neuronal responses observed here are congruent with results reported previously (So et al. 2012; McConnell et al. 2012; McConnell et al. 2016), and match well with clinical observations of frequency-dependent alleviation of motor symptoms during STN DBS (Rizzone et al. 2001; Moro et al. 2002; Fogelson et al. 2005). The suppression of pathological turning in rats during high frequency DBS was correlated with stimulation frequency-dependent sustained increase in neuronal oscillations at the stimulation frequency in both the GPe and SNr. The elevated oscillatory power at steady state during high frequency DBS indicates increased synchronization of neuronal firing to the stimulation pulses, and suggests that this continuous entrainment of neuronal firing to the stimulus pulses is responsible for persistent changes in behavior. Taken together, our results show that distinct mechanisms are responsible for transient and steady-state effects of STN DBS in hemiparkinsonian rats, and suggest that different neural mechanisms may contribute to the immediate and persistent effects of DBS.

Supplementary Material

Refer to Web version on PubMed Central for supplementary material.

Acknowledgments

This work was supported by grants from the US National Institutes of Health (NIH R01 NS040894; NIH R37 NS040894; NIH T32 NS051156), and by the Singapore A*STAR BS-PhD National Science Scholarship. We thank Dr. Justin Hilliard for technical assistance with behavioral analysis, Auriel August for assistance with histology, and Gilda Mills for laboratory support.

References

Burbaud P, Gross C, Bioulac B. Effect of subthalamic high frequency stimulation on substantia nigra pars reticulata and globus pallidus neurons in normal rats. Brain Research. 1994; 14:359–361.

Cooper SE, Noecker AM, Abboud H, Vitek JL, McIntyre CC. Return of bradykinesia after subthalamic stimulation ceases: relationship to electrode location. Exp Neurol. 2011; 231:207–213. [PubMed: 21736878]

Ferensczi E, Deisseroth K. When the electricity (and the lights) go out: transient changes in excitability. Nature Neuroscience. 2012; 15(8):1058–1060. [PubMed: 22837032]

Fogelson N, Kuhn AA, Silberstein P, Limousin PD, Hariz M, Trottenberg T, Kupsch A, Brown P. Frequency dependent effects of subthalamic nucleus stimulation in Parkinson's disease. Neurosci Letters. 2005; 382(1–2):5–9.

Gradinaru V, Mogri M, Thompson K, Henderson J, Deisseroth K. Optical deconstruction of parkinsonian neural circuitry. Science. 2009; 324:354–359. [PubMed: 19299587]

Iribe Y, Moore K, Pang KC, Tepper JM. Subthalamic stimulation-induced synaptic responses in substantia nigra pars compacta dopaminergic neurons in vitro. Journal of Neurophysiology. 1999; 82(2):925–33. [PubMed: 10444687]

Jensen AL, Durand DM. High frequency stimulation can block axonal conduction. Experimental Neurology. 2009; 220(1):57–70. [PubMed: 19660453]

Keresztenyi Z, Valkovic P, Eggert T, Steude U, Hermsdorfer J, Laczko J, Botzel K. The time course of the return of upper limb bradykinesia after cessation of subthalamic stimulation in Parkinson's disease. Parkinsonism Relat Disord. 2007; 8:438–442.

Kuriyama K, Kurihara E. Correlation between rotational behaviors and neurochemical changes associated with damage of rat striatum: Analysis using unilateral microinjection of kainic acid. Neurochemistry International. 1982; 4(6):551–555. [PubMed: 20487910]

Lopiano L, Torre E, Benedetti F, Bergamasco B, Perozzo P, Pollo A, Rizzone M, Tavella A, Lanotte M. Temporal changes in movement time during the switch of the stimulators in Parkinson's disease patients treated by subthalamic nucleus stimulation. Eur Neurol. 2003; 50:94–99. [PubMed: 12944714]

Martin GE, Haubrich DR. Striatal dopamine release and contraversive rotation elicited by intranigrally applied muscimol. Nature. 1978; 275:230–231. [PubMed: 567750]

Matsuoka AJ, Rubinstein JT, Abbas PJ, Miller CA. The effects of interpulse interval on stochastic properties of electrical stimulation: models and measurements. IEEE Trans Biomed Eng. 2001; 48(4):416–24. [PubMed: 11322529]

McConnell GC, So RQ, Hilliard JD, Lopomo P, Grill WM. Effective deep brain stimulation suppresses low-frequency network oscillations in the basal ganglia by regularizing neural firing patterns. Journal of Neuroscience. 2012; 32(45):15657–15668. [PubMed: 23136407]

McConnell GC, So RQ, Grill WM. Failure to suppress low-frequency neuronal oscillatory activity underlies the reduced effectiveness of random patterns of deep brain stimulation. Journal of Neurophysiology. 2016; 115(6):2791–2802. [PubMed: 26961105]

Meissner W, Harnack D, Paul G, Reum T, Sohr R, Morgenster R, Kupsch A. Deep brain stimulation of subthalamic neurons increases striatal dopamine metabolism and induces contralateral circling in freely moving 6-hydroxydopamine-lesioned rats. Neuroscience Letters. 2002; 328(2):105–108. [PubMed: 12133566]

Mitra, PP.; Bokil, H. Observed Brain Dynamics. Oxford University Press; 2008.

Moran A, Stein E, Tischler H, Belelovsky K, Bar-Gad I. Dynamic stereotypic responses of Basal Ganglia neurons to subthalamic nucleus high-frequency stimulation in the parkinsonian primate. Frontiers in Systems Neuroscience. 2011; 5:21. [PubMed: 21559345]

Moro E, Esselink RJ, Xie J, Hommel M, Benabid AL, Pollak P. The impact on Parkinson's disease of electrical parameter settings in STN stimulation. Neurology. 2002; 59:706–713. [PubMed: 12221161]

Moro E, Lozano AM, Pollak P, Agid Y, Rehncrona S, Volkmann J, Kulisevsky J, Obeso JA, Albanese A, Hariz MI, Quinn NP, Speelman JD, Benabid AL, Fraix V, Mendes A, Welter ML, Houeto JL, Cornu P, Dormont D, Tornqvist AL, Ekberg R, Schnitzler A, Timmermann L, Wojtecki L, Gironell A, Rodriguez-Oroz MC, Guridi J, Bentivoglio AR, Contarino MF, Romito L, Scerrati M, Janssens M, Lang AE. Long-term results of a multicenter study on subthalamic and pallidal stimulation in Parkinson's disease. Movement Disorders. 2010; 25:578–586. [PubMed: 20213817]

Nowak K, Mix E, Gimsa J, Strauss U, Sriperumbudur KK, Benecke R, Gimsa U. Optimizing a rodent model of Parkinson's disease for exploring the effects and mechanisms of deep brain stimulation. Parkinson's Disease. 2011; 2011:414682.

Rizzone M, Lanotte M, Bergamasco B, Tavella A, Torre E, Faccani G, Melcarne A, Lopiano L. Deep brain stimulation of the subthalamic nucleus in Parkinson's disease: effects of variation in stimulation parameters. J Neurol Neurosurg Psychiatry. 2001; 71:215–219. [PubMed: 11459896]

Shi LH, Luo F, Woodward DJ, Chang JY. Basal ganglia neural responses during behaviorally effect deep brain stimulation of the subthalamic nucleus in rats performing a treadmill locomotion test. Synapse. 2006; 59(7):445–57. [PubMed: 16521122]

Smith Y, Bolam JP. The output neurons and the dopaminergic neurons of the substantia nigra receive a GABA-containing input from the globus pallidus in the rat. Journal of Comparative Neurology. 1990; 296(1):47–64. [PubMed: 1694189]

So RQ, McConnell GM, Hilliard JD, Grill WM. Characterizing effects of subthalamic nucleus deep brain stimulation on methamphetamine-induced circling behavior in hemiparkinsonian rats. IEEE Transactions on Neural System Rehabilitation Engineering. 2012; 20:626–635.

Spieles-Engemann AL, Collier TJ, Sortwell CE. A functionally relevant and long-term model of deep brain stimulation of the rat subthalamic nucleus: advantages and considerations. European Journal of Neuroscience. 2010; 32(7):1092–9. [PubMed: 21039948]

Summerson SR, Aazhang B, Kemere CT. Characterizing motor and cognitive effects associated with deep brain stimulation in the GPi of hemi-Parkinsonian rats. IEEE Trans Neural Syst Rehabil Eng. 2014; 22(6):1218–27. 2014 Nov. [PubMed: 24951705]

Temperli P, Ghika J, Villemure JG, Burkhard PR, Bogousslavsky J, Vingerhoets FJG. How do parkinsonian signs return after discontinuation of subthalamic DBS? Neurology. 2003; 60:78–81. [PubMed: 12525722]

Ungerstedt U, Arbuthnott GW. Quantitative recording of rotational behavior in rats after 6-hydroxy-dopamine lesions of the nigrostriatal dopamine system. Brain research. 1970; 24(3):485–493. [PubMed: 5494536]

Urbano FJ, Leznik E, Llinas RR. Cortical activation patterns evoked by afferent axons at different frequencies: an in vitro voltage-sensitive dye imaging study. Thalamus & Related Systems. 2002; 1:371–378.

Highlights

- High frequency STN DBS resulted in transient circling contralateral to the lesion
- High frequency STN DBS elicited transient changes in activity of GPe and SNr neurons.
- Distinct mechanisms were responsible for transient and sustained responses.

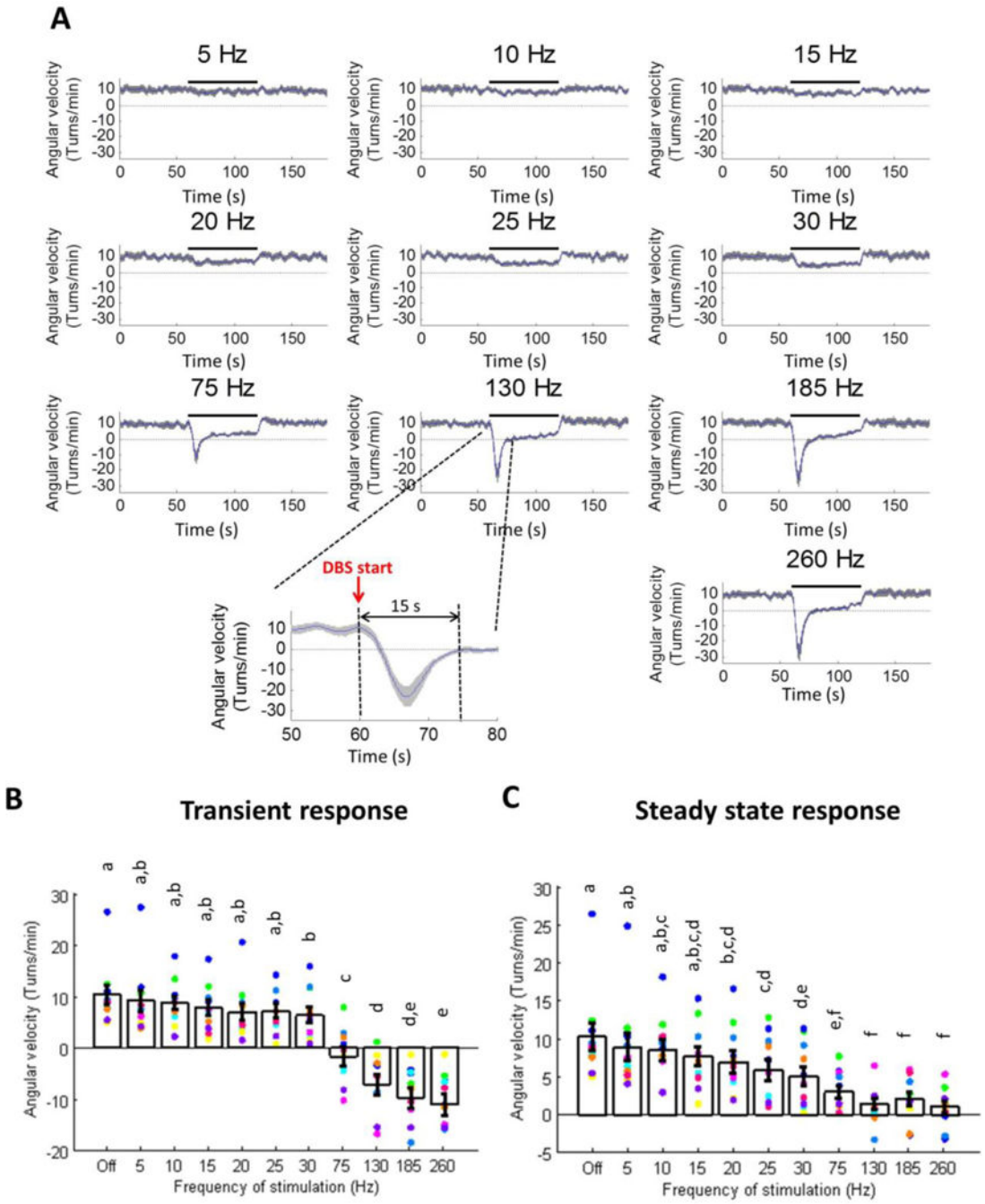

Figure 1.

Transient and steady-state changes in methamphetamine-induced circling during different frequencies of STN DBS (n=11 rats; mean ± SE shown; dots of various colors represent individual rats). **(A)** Angular velocity as a function of time, averaged across rats, where positive values indicate turns ipsilateral to the lesion and negative values indicate turns contralateral to the lesion. **(B)** Quantification of transient (0–15 s after DBS on) angular velocity. Transient response occurred only at frequencies of ≥ 30 Hz ($p < 0.0001$, one-way repeated measures ANOVA). Groups that do not share at least one of the same letter are

significantly different from one another ($p < 0.05$, post-hoc Fisher's PLSD). **(C)** Quantification of steady-state (15–60 s after DBS on) angular velocity. Steady-state angular velocity decreased progressively with increased DBS frequency, and frequencies ≥ 130 Hz resulted in greatest suppression of ipsilateral turning ($p < 0.0001$, one-way repeated measures ANOVA). Groups that do not share at least one of the same letter are significantly different from one another ($p < 0.05$, post-hoc Fisher's PLSD). Data points in B and C show results from individual rats; data from the same rat are indicated by the same color.

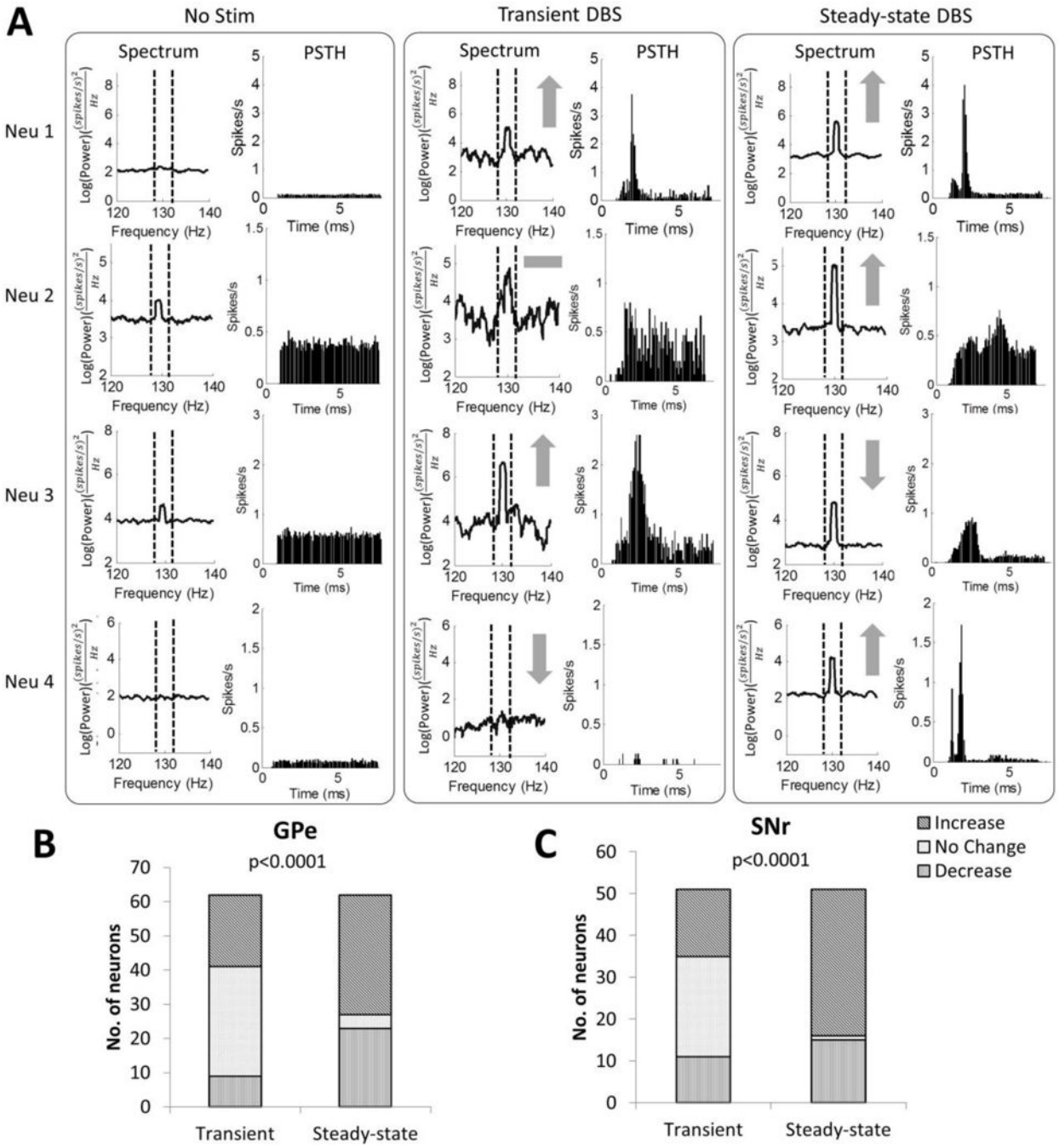

Figure 2.

Transient and steady-state changes in neural oscillatory activity at the stimulus frequency during 130 Hz STN DBS. **(A)** Example responses of single units during the transient and steady-state phases of 130 Hz DBS. Power spectra and post-stimulus histograms (PSTH) of four example neurons (neuron 1 from GPe, neurons 2–4 from SNr) before DBS, during the transient phase (0 – 15 s after DBS on) of 130 Hz DBS, and during the steady-state phase (15 – 60 s after DBS on) of 130 Hz DBS are shown. Gray symbols indicate increase (↑), decrease(↓), and no change (−) in oscillatory power at the stimulation frequency compared

to baseline. **(B)** Proportion of GPe neurons with increased, no change, or decreased 130 Hz oscillatory power during the transient and steady-state phases of 130 Hz DBS. **(C)** Proportion of SNr neurons with increased, no change, or decreased 130 Hz oscillatory power during the transient and steady-state phases of 130 Hz DBS (*p* values from Pearson's chi-squared test of differences in proportions between the transient and steady-state phases).

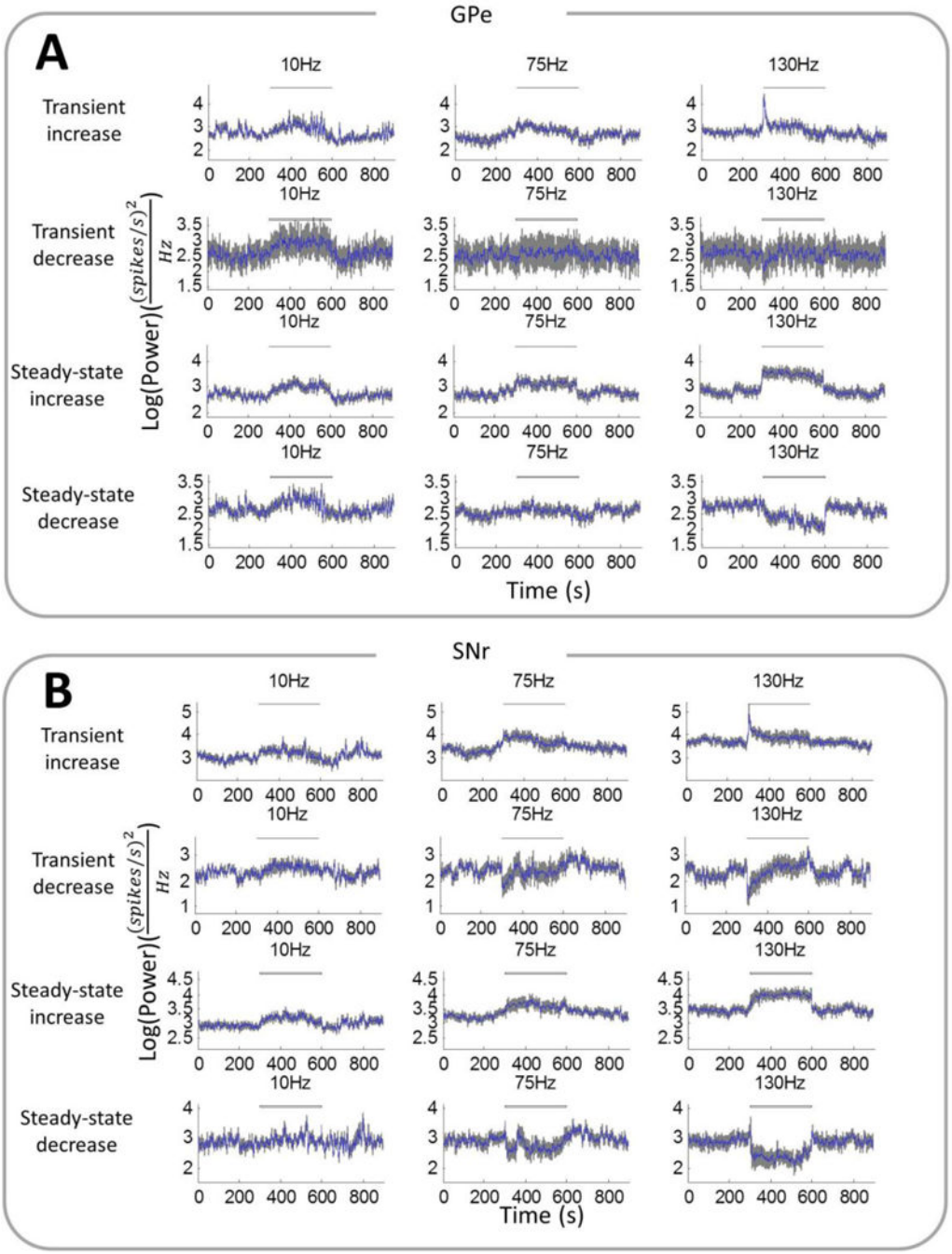

Figure 3.

Oscillatory power at the stimulation frequency (± 1 Hz) in the firing times of single units in the (**A**) GPe and (**B**) SNr before, during, and after different frequencies of STN DBS. Power was averaged (mean ± SE) across subsets of single units in the GPe and SNr that exhibited transient increase (GPe: n=21; SNr: n=16), transient decrease (GPe: n=9; SNr: n=11), steady-state increase (GPe: n=35; SNr: n=35) or steady-state decrease (GPe: n=23; SNr: n=15) in oscillatory power during 130 Hz DBS.

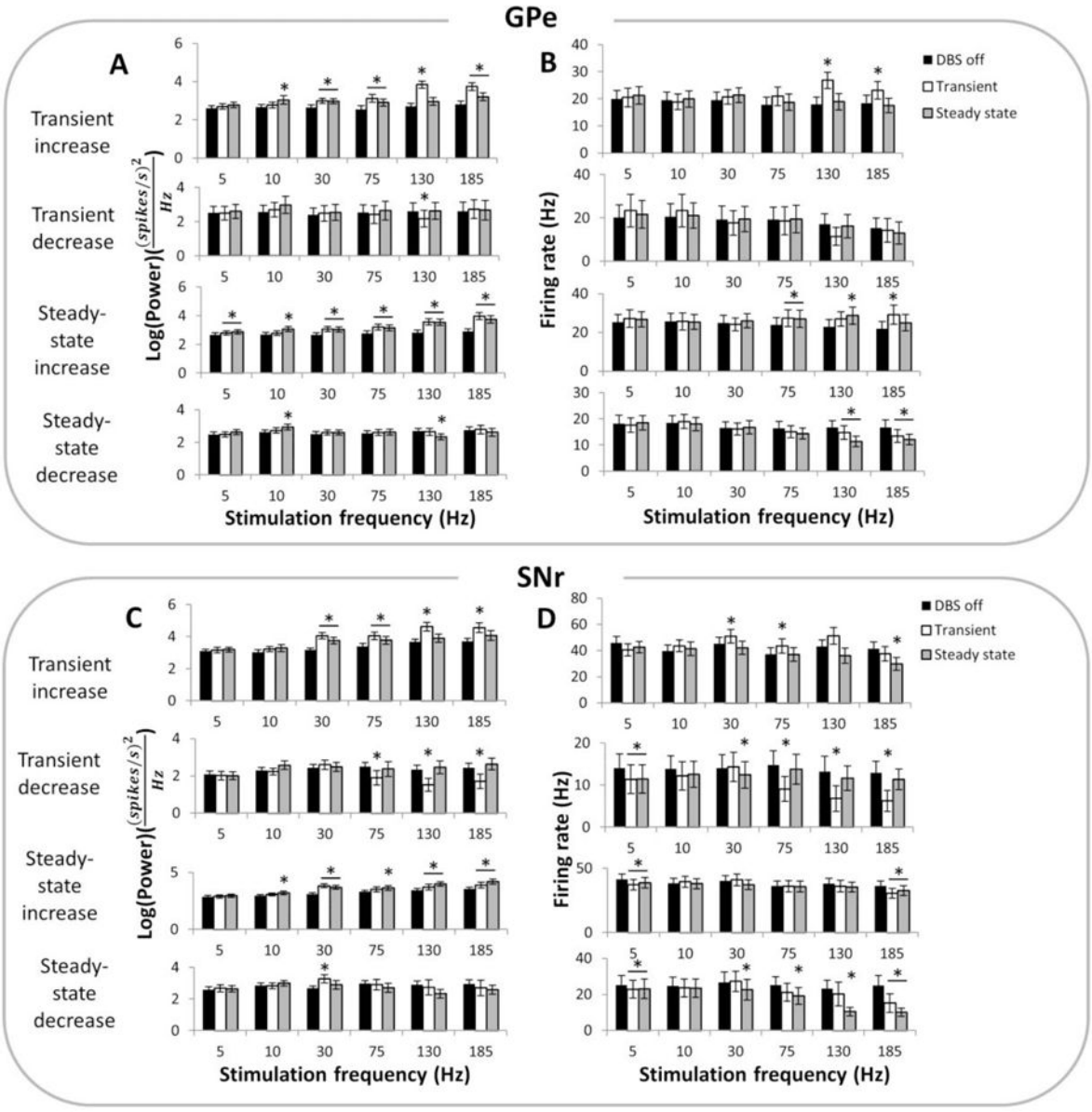

Figure 4.

(A) Quantification of changes in oscillatory power in the GPe at the stimulation frequency during DBS off, during the transient phase after onset of DBS or and during the steady-state phase of DBS, at different frequencies of stimulation. Oscillatory power was quantified for subsets of single units in the GPe that exhibited transient increase (n=21), transient decrease (n=9), steady-state increase (n=35) or steady-state decrease (n=23) in oscillatory power during 130 Hz DBS **(B)** Quantification of changes in firing rates in the same subset of GPe neurons as in (A) during different frequencies of DBS. **(C)** Quantification of changes in oscillatory power in the SNr at the stimulation frequency during DBS off, transient DBS or steady-state DBS, at various frequencies of stimulation. Oscillatory power was quantified for subsets of single units in the SNr that exhibited transient increase (n=16), transient decrease (n=11), steady-state increase (n=35) or steady-state decrease (n=15) in oscillatory power

during 130 Hz DBS. **(D)** Quantification of changes in firing rates in the same subset of SNr neurons as in (C) during different frequencies of DBS. (*) indicates a significant difference from DBS off ($p < 0.05$, one-way repeated measures ANOVA and post-hoc Fisher's PLSD).

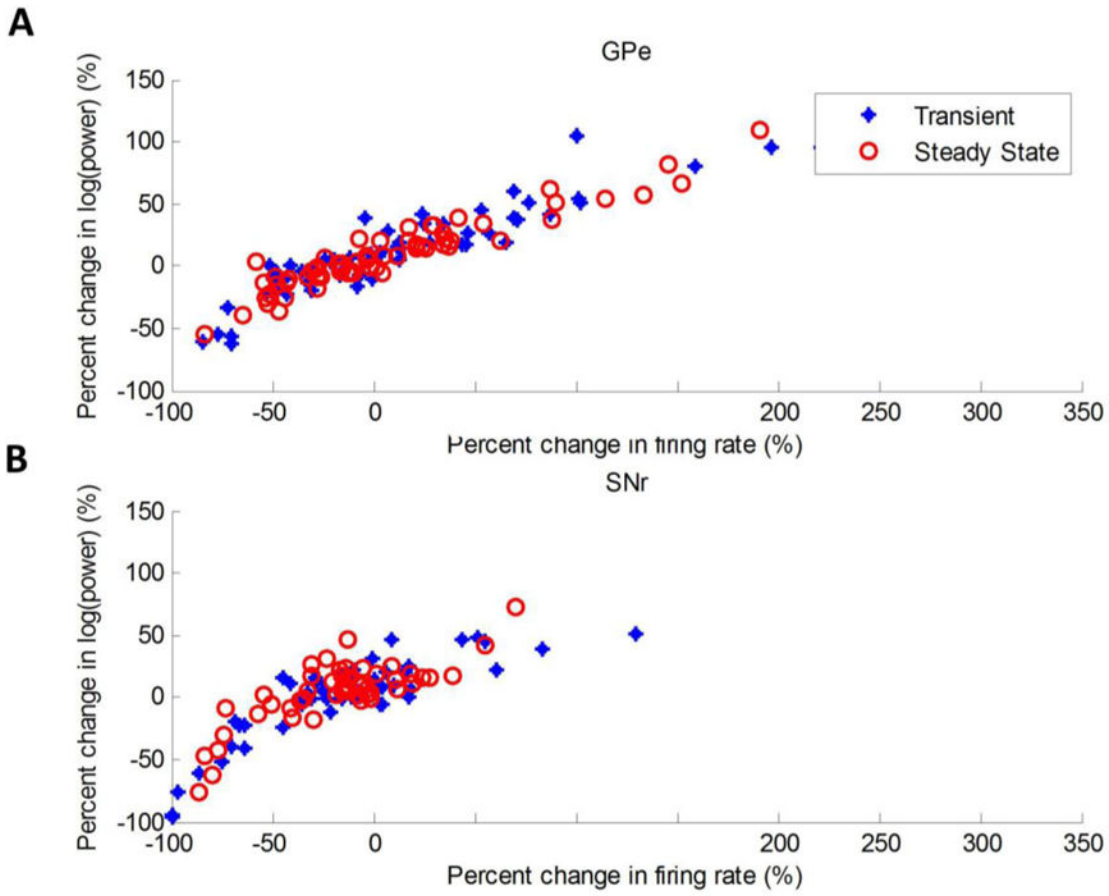

Figure 5.

Pearson's linear correlation coefficient (r) was used to quantify correlation between percent change in firing rate and percent change in 130 Hz oscillatory power during the transient and steady-state phases of 130 Hz DBS in **(A)** the GPe (transient: $r = 0.9169$, $p < 0.001$; steady-state: $r = 0.9462$, $p < 0.001$) and **(B)** the SNr (transient: $r = 0.8561$, $p < 0.001$; steady-state: $r = 0.7958$, $p < 0.001$).